International Journal of Remote Sensing

ISSN: 0143-1161 (Print) 1366-5901 (Online) Journal homepage: https://www.tandfonline.com/loi/tres20

Testing two methods for mapping water hyacinth (*Eichhornia crassipes*) in the Greater Letaba river system, South Africa: discrimination and mapping potential of the polar-orbiting Sentinel-2 MSI and Landsat 8 OLI sensors

Kgabo Humphrey Thamaga & Timothy Dube

To cite this article: Kgabo Humphrey Thamaga & Timothy Dube (2018) Testing two methods for mapping water hyacinth (*Eichhornia crassipes*) in the Greater Letaba river system, South Africa: discrimination and mapping potential of the polar-orbiting Sentinel-2 MSI and Landsat 8 OLI sensors, International Journal of Remote Sensing, 39:22, 8041-8059, DOI: 10.1080/01431161.2018.1479796

To link to this article: https://doi.org/10.1080/01431161.2018.1479796

INTERNATIONAL JOURNAL OF REMOTE SENSING
2018, VOL. 39, NO. 22, 8041–8059
https://doi.org/10.1080/01431161.2018.1479796

Taylor & Francis
Taylor & Francis Group

Testing two methods for mapping water hyacinth (*Eichhornia crassipes*) in the Greater Letaba river system, South Africa: discrimination and mapping potential of the polar-orbiting Sentinel-2 MSI and Landsat 8 OLI sensors

Kgabo Humphrey Thamaga [a] and Timothy Dube [b]

[a]Department of Geography and Environmental Studies, University of Limpopo, Polokwane, South Africa; [b]Department of Earth Sciences, University of the Western Cape, Bellville, South Africa

ABSTRACT

Early detection and mapping of the spatio-temporal distribution of invasive water hyacinth (*Eichhornia crassipes*) in inland hydrological systems are vital for a number of water resource management-related reasons. Field surveys and current climate change projections (associated with longer dry spells, and shortened rain seasons) have shown that climate change and the rapid spread of aquatic invasive species are increasingly affecting inland surface water availability in semi-arid regions of Southern Africa. It is upon this premise that accurate, reliable, and timely information on the spatio-temporal distribution and configuration of water hyacinth is required in tracing their evolution and propagation in affected areas as well as in potential vulnerable areas. This work, therefore, attempts to test two robust push-broom multispectral sensors: Landsat 8 Operational Land Imager (OLI) and Sentinel-2 MultiSpectral Instrument (MSI) in identifying, detecting, and mapping the spatial distribution and configuration of invasive water hyacinth in a river system. The results of the study show that water hyacinth in small reservoirs can be mapped with an overall accuracy of 68.44% and 77.56% using Landsat 8 and Sentinel-2 data, respectively. The results further demonstrated the blue, red, red edge (RE) 1, short-wavelength infrared (SWIR)-1, and SWIR-2 of both satellite data sets as the critical and outstanding spectral regions in detecting and mapping water hyacinth from other land-cover types. Overall, the study highlights the unexploited prospects of the new noncommercial multispectral sensors in monitoring invasive species infestation from inland surface waterbodies in semi-arid regions (i.e. smaller reservoirs).

ARTICLE HISTORY
Received 27 November 2017
Accepted 8 May 2018

1. Introduction

Sub-Saharan Africa and other parts of the developing world currently face the largest wave of urban growth and industrial revolution in history (Mendes, Bertella, and Teixeira 2014). Amongst other factors, the fast urban growth, together with the rural-to-urban

CONTACT Kgabo Humphrey Thamaga hkgaboreba@gmail.com Department of Geography and Environmental Studies, University of Limpopo, Private Bag X1106, Sovenga, Polokwane 0727, South Africa

migration, generates continuous expansion of slums (e.g. approximately 70% of African urban dwellers live in slums) which cannot cope with the provision of proper sanitation infrastructures (Potts 2013; Krishna, Siram, and Prakash 2014; Rigg, Nguyen, and Luong 2014; APHRC 2014). Chawira, Dube, and Gumindoga (2013) noted that rural-to-urban migration and uncontrolled city growth have led to heavy urban water pollution (microbial and nutrient) via the discharge of poorly treated municipal wastewater in the freshwater ecosystem. Microbial and chemical freshwater pollution end up being deposited in surrounding waterbodies leads to water eutrophication and the proliferation of aquatic weeds. Previous work shows that the spread of aquatic weeds in most freshwater bodies is linked to a number of land management practices (e.g. fertilizers or nutrients), as well as poor and uncontrolled discharge of sewage to river systems that create a conducive breeding ground for the growth of undesirable species (Chawira, Dube, and Gumindoga 2013; Giardino et al. 2015). In addition to nutrient concentrations, the spatial distribution and spread of these species are also influenced by environmental factors, such as depth of the river, topography, type of soil substrates, water turbidity, as well as exposure to wind (Pearsall 1920; Rorslett 1984; Harvey, Pickett, and Bates 1987). Any changes in climatic conditions are most likely to alter the plant distribution and function (Shoko and Mutanga 2017).

Aquatic weed infestation is one of the major environmental challenges globally, threatening the integrity and functioning of most hydrological ecosystems (Cheruiyot et al. 2014). Moreover, the current projected climate change associated with longer dry spells and shortened rain seasons coupled with the rapid spread of aquatic invasive species is likely to make inland water reservoirs in Southern Africa even much drier and scarce (Midgley et al., 2015). Continuous observation and monitoring of the proliferation of aquatic weeds are thus essential for proper water resource management and for the development of appropriate weed control strategies and prioritizations of most infested areas (Albright, Moorhouse, and McNabb 2004). To date, this environmental problem has received limited attention from the responsible hydrologists, environmentalists, and researchers, due to either limited financial resources or the lack of technical expertise (Dube, Gumindoga, and Chawira 2014), assurance in product accuracy and high-resolution satellite data continuity, and, in some instances, the lack of government will or prioritization.

Despite the presence of these barriers, there are clear breakthroughs or inroads in remote-sensing applications in water quality-related studies (Bresciani et al. 2011; Bonansea et al. 2015; Masocha et al., 2016), wetland vegetation mapping (Huang et al. 2014; Li et al., 2005; Jin et al. 2017), and aquatic invasive alien species, especially in large reservoirs (Dronova, Gong, and Wang 2011). Unlike conventional field surveys, remotely sensed data are the key primary data source for mapping and monitoring the functioning and rate of invasion of hydrological systems, as well as identifying potential vulnerable areas, especially in developing countries, given the scarcity in ground data or lack of data access, due to institutional restrictions. Although there is limited appreciation of this technology by policy and decision-makers in Africa, its relevance remains unquestionable.

Developing accurate, spatially explicit, fine-scale records on rates of invasions is a high priority (Panetta and Lawes 2005). Therefore, remote-sensing technologies emerge as a reliable approach in studying aquatic ecosystems. The availability of satellite data provides great potential for the spatial and temporal monitoring of aquatic weeds in a timely and cost-effective approach. Recent studies utilized remotely sensed data in monitoring lake

conditions, due to their expansive nature (McCullough et al., 2012; Hou et al. 2017). Broadband multispectral sensors have demonstrated success in monitoring these areas (Dube, Gumindoga, and Chawira 2014; Giardino et al. 2015; Shekede, Kusangaya, and Schmidt 2008). However, little consideration has been paid in monitoring invasive water hyacinth in complex environments, such as smaller rivers, using these sensors. Satellite remote sensing of small freshwater systems has been limited by the sensing characteristics, in terms of spectral, radiometric, temporal, and more importantly spatial (Hestir et al. 2015). Past noncommercial satellite missions could not provide appropriate measurement resolutions needed to fully resolve freshwater ecosystem properties and processes (Hestir et al. 2015). Due to the presence of mixed or ecological overlap of plant species in aquatic ecosystems, discriminating aquatic weeds from other aquatic plants remains a challenge, as it requires moderate to high spatial and spectral resolutions, in both visible and shortwave infrared regions (Hestir et al. 2008). This problem is also supported by Cheruiyot et al. (2014) who stated that although multispectral remote sensing has the capability to detect and map alien plants, the weeds are often obscured in a backdrop of natural vegetation, making it difficult to be detected or even mapped at a fine-scale. In this case, sensors with high spatial, spectral, temporal, and radiometric resolutions are needed on a broader scale for accurate ecological monitoring to understand water hyacinth distribution and to enhance management practices on both open and complex environments.

Although the previous satellite products have been associated with limitations in mapping aquatic invasive species, new crop of noncommercial sensors, e.g. Landsat 8 Operational Land Imager (OLI) and Sentinel-2 MultiSpectral Instrument (MSI), with improved sensing characteristics has demonstrated promising prospects in vegetation mapping (Fu 2003; Zhang et al. 2016). These sensors also show some potential for land-use and land-cover mapping (Kaufmann and Stern 1997; Hassan et al. 2016), biomass estimation (Yavaşl 2016), and plant and crop disease monitoring (Hillnhutter and Mahleni 2008; Dhau et al. 2017). For instance, Shoko and Mutanga (2017) demonstrated the unique capability of the newly launched Sentinel-2 MSI sensor in detecting and discriminating subtle differences between C3 and C4 grass species with an overall classification accuracy of 90.41%. These sensors are, therefore, perceived to provide new and invaluable opportunities for detecting, mapping, monitoring, and understanding the proliferation of water hyacinth in smaller reservoirs – a previously challenging task with broadband multispectral satellite data. Refined sensing characteristics, which include the high spatial resolution (±10 m) and the presence of new and strategically positioned spectral waveband red edge (RE), previously a characteristic of high-resolution commercial sensors, e.g. Worldview 2, IKONOS etc., bring with its unique improvements that could enable subtle detection and discrimination of aquatic weeds often obscured in the backdrop of natural vegetation. Besides, the greater and free availability of remotely sensed data at higher spatial and spectral resolutions coupled with the development of machine-learning algorithms could potentially improve classification accuracies which maybe a great step towards water resource management (Peerbhay, Mutanga, and Ismail 2016). Therefore, this study sought to test the capability of Landsat 8 OLI and Sentinel-2 MSI sensors in detecting and mapping the spatial distribution and configuration of invasive water hyacinth (*Eichhornia crassipes*) in the Greater Letaba river system in Tzaneen, South Africa.

2. Materials and methods

2.1. *Study area*

The study was conducted at the Greater Letaba river system in Tzaneen, South Africa. The area is located at −23° 39.036′S, 31° 9.006′E (Figure 1). The Greater Letaba river system is the main freshwater supply for the neighbouring communities and farmlands in Tzaneen area. The river system has been affected by a widespread invasion by water hyacinth (*E. crassipes*) and has deteriorated by continuous accretion of fertilizers from the surrounding farmlands carried out through run-off and disposal of raw sewage from the surrounding urban areas. The area has a mean annual temperature of 28°C and mean annual precipitation of 612 mm (DEAT 2001). The main land-cover types within the study area include croplands, grasslands, fruit trees, built up, roads, and plantation (DEAT 2001). Commercial farming is the dominant human activity in the area.

2.2. *Field survey and preprocessing*

The capability of Landsat 8 OLI and Sentinel-2 MSI was tested in discriminating water hyacinth from other coexisting land-cover types, such as bare land, plantation, and riparian vegetation, other vegetation, water, as well as built up. Field data collection was conducted to record the location of water hyacinth and other land-cover classes, at sub-metre accuracy, using Global Position System (GPS). Field data were collected from 24 June to 26 June 2017. Field data collection was achieved, using randomly generated sampling points across the river system, using the Hawths Analysis Tool in ArcGIS 10.4 software (ESRI, Redlands, CA, USA). A total of

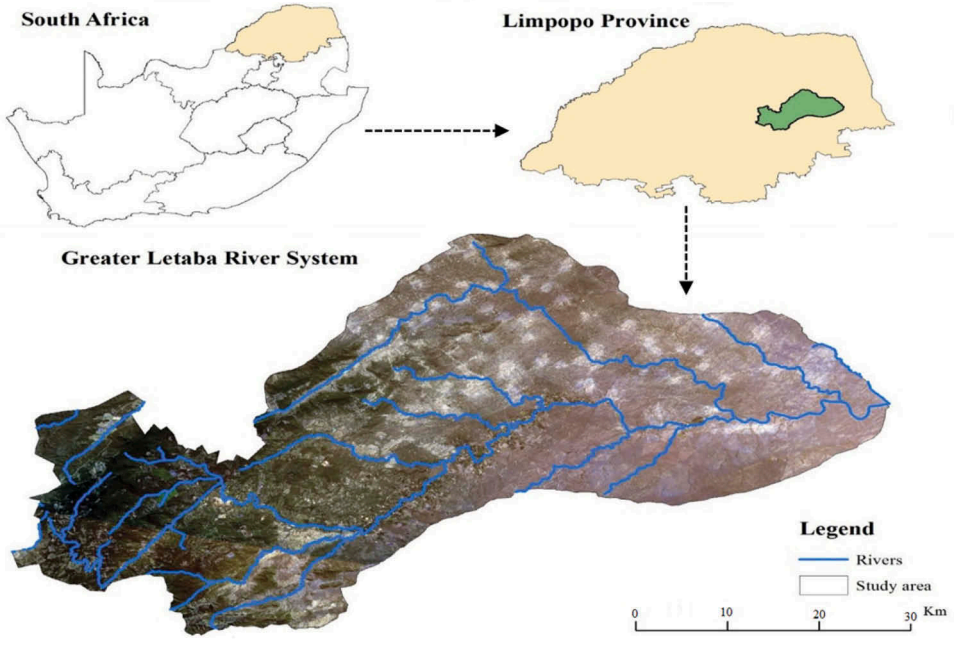

Figure 1. Map showing location of the study area.

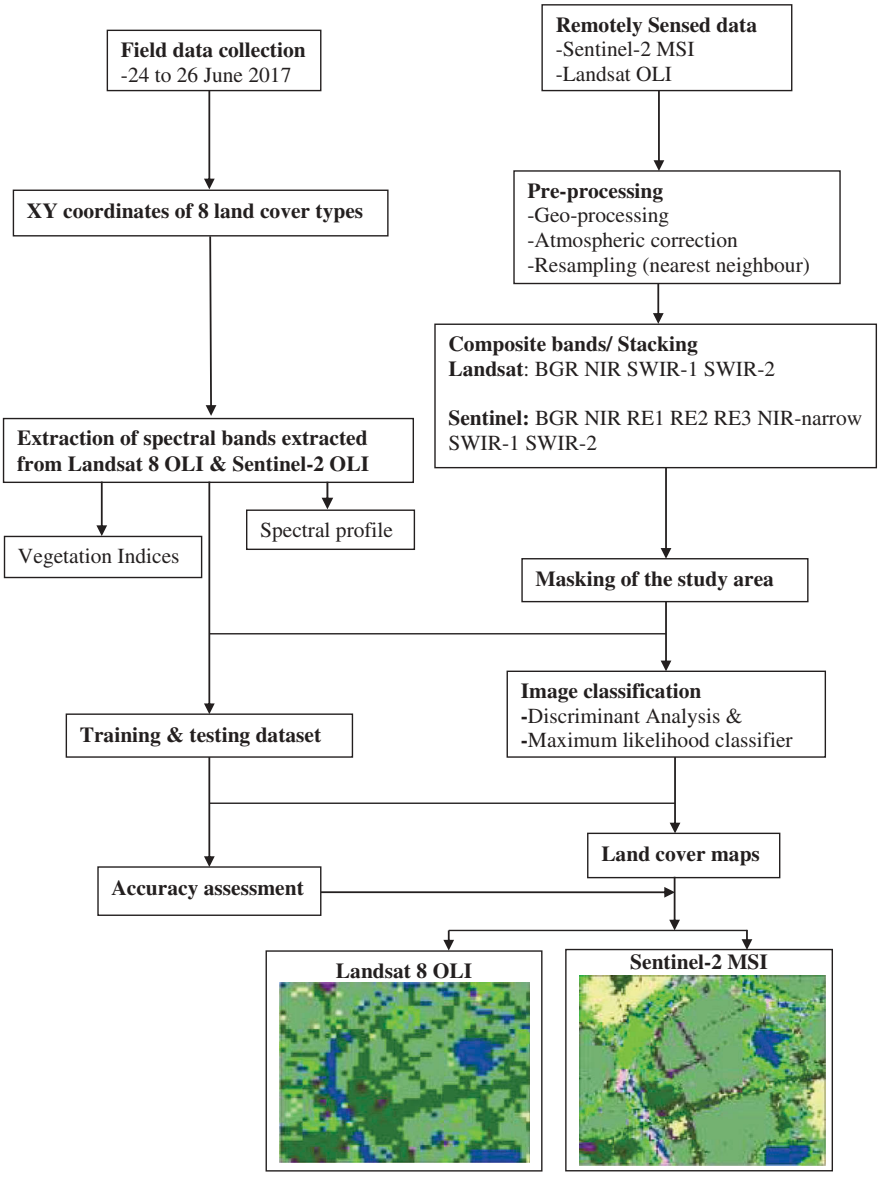

Figure 2. Flow chart of method.

329 points (47 points per land-cover type) were generated, and these were used to discriminate water hyacinth from other land-cover types. Ground-truthing measurements coinciding with satellite image acquisition period were used. In the present study, correspondence principle for image acquisition and ground-truthing measurements was set to 3 days. The period allows for adequate matchups between ground-truth data and satellite imagery (Sriwongsitanon, Surakit, and Thianpopirug 2011; Tebbs, Remedios, and Happer 2013; Lamaro, Mariñelarena, and Torrusio. 2013). Sites of recorded land-cover types, using GPS, were then imported into ArcGIS 10.4 software environment for classification purposes.

2.3. *Remote-sensing data acquisition and preprocessing*

Sentinel-2 MSI and Landsat 8 OLI remotely satellite images were acquired to test the sensors' capability in discriminating water hyacinth from other vegetation cover types. Detailed spectral and spatial information on the satellite images used for analysis are presented in Table 1. Both cloudless satellite images covering the Greater Letaba river system were freely acquired from the online Landsat and Sentinel series archive manned by the United States Geological Survey (USGS) website. The satellite images were acquired between 24 June and 26 June 2017 with two tiles of Landsat 8 OLI and six tiles of Sentinel-2 MSI covering the study area. Satellite images were then atmospherically corrected using Dark Object Subtraction (DOS1) model under Semi-Automated Classification (SCP) embedded in Quantum GIS (QGIS Development Team, Amsterdam, Netherlands) 2.18.03 software. Preprocessing was done, using QGIS software to convert all the image bands into reflectance. We then resampled spectral bands of Sentinel-2 MSI from 20 m to 10 m using nearest neighbour resampling method. All tiles in both sensors were mosaicked using ArcGIS 10.4 to cover the extent of the study area. The 329 field-sampled points were then overlaid on the layer-stacked reflectance images to extract the corresponding reflectance values. The extracted reflectance values per spectral band were then exported as a table in Microsoft excel. The data were then used to calculate spectral vegetation indices (Table 2). The selected indices were chosen based on their capabilities in improving vegetation spectral responses (Pahlevan and Schott 2013; El-Askary et al. 2014). For classification accuracy assessment, there is a disagreement between proportions of testing and training sets of land-cover types. Before proceeding with the analysis, the extracted spectral reflectance was randomly divided into 30% testing and 70% training sets, which is a requirement for all machine-learning algorithms (Adjorlolo et al. 2013; Adelabu et al. 2014; Sibanda, Mutanga, and Rouget 2015).

2.4. *Water hyacinth mapping using the discriminant analysis (DA)*

A variety of classification algorithms have been developed and used to map the spatial distribution of invasive water hyacinth in the freshwater ecosystem. In this study, we used DA to test the capability of new-generation sensors Landsat 8 OLI and Sentinel-2 MSI data in mapping water hyacinth radiance from other land-cover types. The choice of the model was based on its performance in classification as reported in previous studies

Table 1. Sensors spectral and spatial characteristics of Landsat OLI and Sentinel-2 MSI.

Landsat 8 OLI			Santinel-2 MSI		
Band	Band width	Resolution (m)	Band	Band width	Resolution (m)
Blue	0.45–0.52	30	Blue	0.49	10
Green	0.53–0.60	30	Green	0.56	10
Red	0.63–0.68	30	Red	0.67	10
NIR	0.85–0.89	30	RE 1	0.71	20
SWIR-1	1.56–1.66	30	RE 2	0.74	20
SWIR-2	2.10–2.30	30	RE 3	0.78	20
			NIR	0.84	10
			SWIR-1	0.16	20
			NIR narrow	0.87	20
			SWIR-1	0.16	20
			SWIR-2	0.22	20

NIR: near infrared; SWIR: shorter wave infrared; RE: red edge.

Table 2. Landsat 8 OLI and Sentinel-2 MSI spectral bands and vegetation indices.

Index	Formula	Reference
NDVI	(NIR − Red)/(NIR + Red)	Tucker (1979)
NDWI	(Green − NIR)/(Green + NIR)	McFeeters (1996)
EVI	2.5 ((NIR − Red)/(1 + NIR + 6Red − 7.5Blue))	Huete et al. 1997
SRI	(NIR/Red)	Jordan (1969)
SAVI	((NIR − Red) (1 + L))/(NIR2 + Red + L)	Huete (1988)
GI	Green/Red	Zarco-Tejeda et al., 2005
GNDVI	(NIR − Green)/(NIR + Green)	Gitelson, Kaufman, and Merzlyak (1996)
Clgreen	(NIR/Green) − 1	Gitelson et al., 2002
ARVI	(NIR − (2(Red − Blue)))/(NIR + (2 (NIR − Blue)))	Kaufman and Tanré 1992
TVI	$\sqrt{(NIR - Red)/(NIR + Red) + 0.5)}$	Deering et al. 1975
OSAVI	(NIR − Red)/(NIR + Red + 0.16)	Rondeaux, Steven, and Baret 1996
RDVI	$\sqrt{(NDVI)(DVI)}$	Roujean and Breon 1995
VGI	(Green − Red)/(Green + Red)	McFeeters (1996)
NG	Green/NIR + Red + Green	Sripada et al. 2006
DVI	NIR − Green	Tucker 1979

NDVI: normalized difference vegetation index; NDWI: normalized difference water index; EVI: enhanced vegetation index; SRI: Simple Ratio Index; SAVI: Soil-Adjusted Vegetation Index; GI: greenness index; GNDVI: green normalized difference vegetation index; Clgreen: Chlorophyll Index Green; ARVI: Atmospherically Resistant Vegetation Index; TVI: Transformed Vegetation Index; OSAVI: optimized soil-adjusted vegetation index; RDVI: renormalized difference vegetation index; VGI: vegetation greenness index; NG: normalized green; DVI: Difference Vegetation Index.

(Sibanda, Mutanga, and Rouget 2015; Matongera et al. 2017; Shoko and Mutanga 2017). Fernandez (2002) describes DA as multivariate statistical classifier used to model group discrimination based on observed predictor variables of remote sensing in each observation into one of the groups. DA uses a linear function (assumes multivariate normality with equivalent covariance matrices) for classification criterion derived from individualities within a set group of covariance matrices. The observations classified within the group discriminate land-cover types into categories based on a measure of generalized squared distance. The algorithm was, therefore, used to classify and derive confusion matrices from the derived water hyacinth maps. The model converts reflectance data of land-cover types at each waveband into several components that account for the difference in reflectance amongst land-cover types (Sibanda, Mutanga, and Rouget 2015). The classification accuracy is formulated (confusion matrix) using an error matrix of predicted (classified) versus known (reference) occurrences of a target (Congalton 1991). Confusion matrix yields estimates of an overall accuracy, user accuracy, and producer accuracy and may also be used to calculate statistical measures of accuracy (i.e. kappa statistics) (Congalton and Green 1999; Foody 2004). To test the capability of sensors in detecting spatial distribution of water hyacinth, Table 3 and Figure 2 illustrate analysis procedures that were implemented in this study. For example, three analytical experiments, (i) spectral bands; (ii) spectral vegetation indices; and (iii) combined

Table 3. Landsat 8 OLI and Sentinel-2 MSI experiments for water hyacinth.

Data type	Sensor	Spectral information	Analysis
Spectral bands (SB)	Landsat 8	Blue, green, red, NIR, SWIR-1, and SWIR-2	I
	Sentinel-2	Blue, green, red, red edge(RE) 1, RE 2, RE 3, NIR, NIR narrow, SWIR-1, and SWIR-2	
Spectral vegetation indices (SVIs)	Landsat 8	NDVI, NDWI, EVI, SRI, SAVI, GI, GNDVI, Clgreen, ARVI, RVI, TVI, OSAVI,	II
	Sentinel-2	RDVI, VGI, NGI, and DVI	
SB + SVIs	Landsat 8	6 bands + 16 SVIs	III
	Sentinel-2	10 bands + 16 SVIs	

spectral and vegetation indices, were applied in Microsoft XL STAT 2013 to generate classification accuracies (overall, user, and producer accuracy).

2.5. *Statistical data analysis*

Prior to statistical analysis, exploratory data analysis was done to understand the data. Analysis of variance (ANOVA) was used to identify spectral separability of water hyacinth amongst other land-cover types. We conducted ANOVA to test if there is significant difference ($\alpha = 0.05$) between water hyacinth and other land-cover types based on the derived spectral data for the two sensors. Windows of spectral separability based on both Landsat 8 OLI and Sentinel-2 MSI were used to test which band(s) can optimally discriminate water hyacinth from other land-cover types.

3. Results

3.1. *Discriminating water hyacinth from other land-cover types*

Figure 3 illustrates the derived spectral profiles for water hyacinth and other land-cover types considered in this study. The spectral profiles were derived using averaged Sentinel-2 MSI- and Landsat 8 OLI (Figure 3(a,b))-derived spectral information. Overall, the results show that water hyacinth can be discriminated from other land-cover types using the SWIR-2 spectral regions of Landsat 8 and blue, SWIR-1, as well as SWIR-2 of Sentinel-2. Sentinel-2 illustrates a clear window of spectral separability on the following bands: blue, RE 1, SWIR-1, and SWIR-2 compared to Landsat 8 OLI.

3.2. *Image classification accuracies*

3.2.1. *Analysis I: water hyacinth classification using raw spectral data*

Figure 4(a,b) illustrates classification accuracies of water hyacinth from other land-cover types derived from Sentinel-2 MSI and Landsat 8 OLI data sets. It was observed that the Sentinel-2 MSI outperformed Landsat 8 OLI in discriminating water hyacinth producing an overall accuracy of 73% when compared to Landsat 8 OLI which yielded a slightly lower overall accuracy of 63.34%, with a deviation of 9.66% (Table 4). Furthermore, Sentinel-2 produced good user and producer accuracies when compared to Landsat 8 OLI. For water hyacinth, Sentinel-2 yielded user accuracy of 78.56% and producer accuracy of 57.89% (Figure 4) when compared to Landsat 8 OLI that yielded low classification accuracies with user accuracy of 20% and producer accuracy of 35.67% (Figure 4). In comparison to other land-cover types, the plantations produced low accuracy with 36.41% in Sentinel-2. Overall, Landsat 8 had the lowest user and producer accuracies as compared to Sentinel 2 sensor.

3.2.2. *Analysis II: water hyacinth classification using Landsat 8- and Sentinel-2-derived vegetation indices*

Water hyacinth classification accuracy using different spectral vegetation indices demonstrated that the difference in sensors slightly improved performances when compared to the use of raw spectral bands. Figure 5(a,b) shows that Sentinel-2 outperformed Landsat

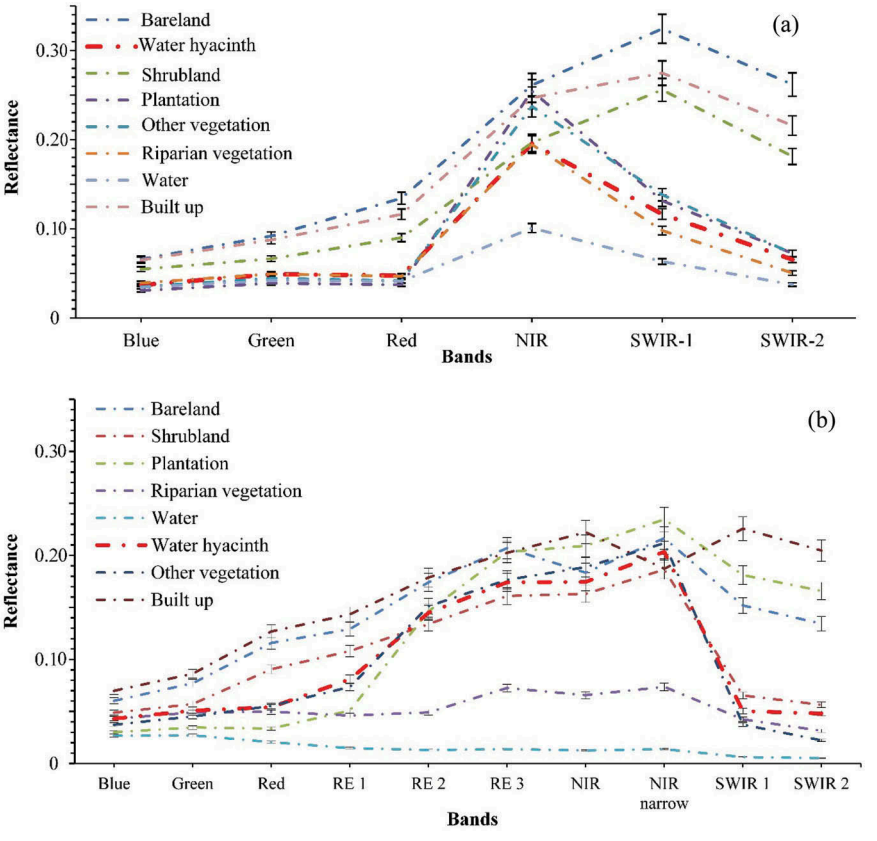

Figure 3. Averaged spectral reflectance for eight land-cover types using: (a) Landsat 8 OLI and (b) Sentinel-2 MSI sensors.

8 in discriminating water hyacinth from other land-cover types producing an overall accuracy of 73.31% (Figure 6). On the other hand, Landsat 8 OLI-derived spectral vegetation indices yielded overall accuracy of 65.53%. Compared to the first analysis (I), Landsat 8 OLI overall accuracy increased by 2.19% (Table 4) and by 0.31% for Sentinel-2. Furthermore, user and producer accuracies increased in both sensors, respectively (Figure 5). Regardless of the increase in user and producer accuracy of water hyacinth in both sensors, Landsat 8 OLI yielded lower accuracies with user accuracy of 40% and producer accuracy of 47.64%. When compared to other land-cover types, plantation and shrub land produced higher classification of 100%.

3.2.3. *Analysis III: water hyacinth classification using combined Landsat 8- and Sentinel-2-derived spectral bands and spectral vegetation indices*

Figure 7 illustrates the classification accuracy of water hyacinth based on integrated data sets of spectral bands and spectral vegetation indices derived from Landsat 8 and Sentinel-2, respectively. The combination of spectral bands and spectral vegetation indices produced satisfactory results for both sensors. For example, Sentinel-2 yielded an improved overall classification accuracy of 77.56% (Figure 6) and, when compared to analysis I, displays an overall improvement in accuracy of 4.56% and 4.25% from analysis II (Table 4). Although

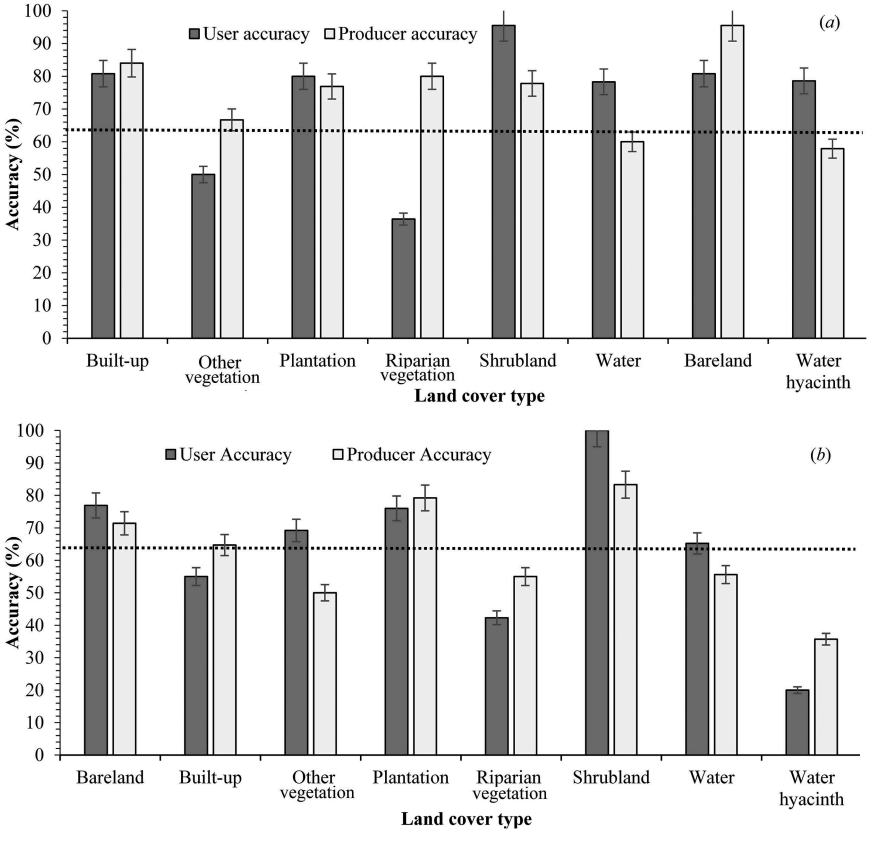

Figure 4. Classification accuracies of water hyacinth and other land-cover types derived from (a) Sentinel-2 and (b) Landsat 8 spectral data set. Dotted line represents good classification accuracies above 65% (Shoko and Mutanga 2017).

Table 4. Deviation of classification accuracies between Sentinel-2 MSI and Landsat 8 OLI.

			Deviations in terms of accuracy (%)		
Sensor	Parameter	Accuracy (%)	I	II	III
Landsat 8 OLI	Bands	63.34	-	−2.19	−5.07
	VIs	65.53	±2.19	-	−2.88
	Bands + VIs	68.41	±5.07	±2.88	-
Sentinel-2 MSI	Bands	73	-	−0.31	−4.56
	VIs	73.31	±0.31	-	−4.25
	Bands + VIs	77.56	±4.56	±4.25	-

overall classification accuracy of Landsat 8 increased by 5.07% from analysis I and 2.88% from analysis II, the combined data sets produced overall accuracy of 68.41% (Figure 6). Integrated data sets produced user accuracy of 89.30% and producer accuracy of 61% for water hyacinth. When compared to analysis I, user accuracy increased by 10.74% whereas the producer accuracy increased by 3.11%; furthermore, when compared to analysis II, user and producer accuracy dropped by 3.11%. From the observation, water hyacinth produced lowest classification accuracies with user accuracy of 44% and producer accuracy of 50% using Landsat 8 OLI. Additionally, we compared the overall classification performance of the

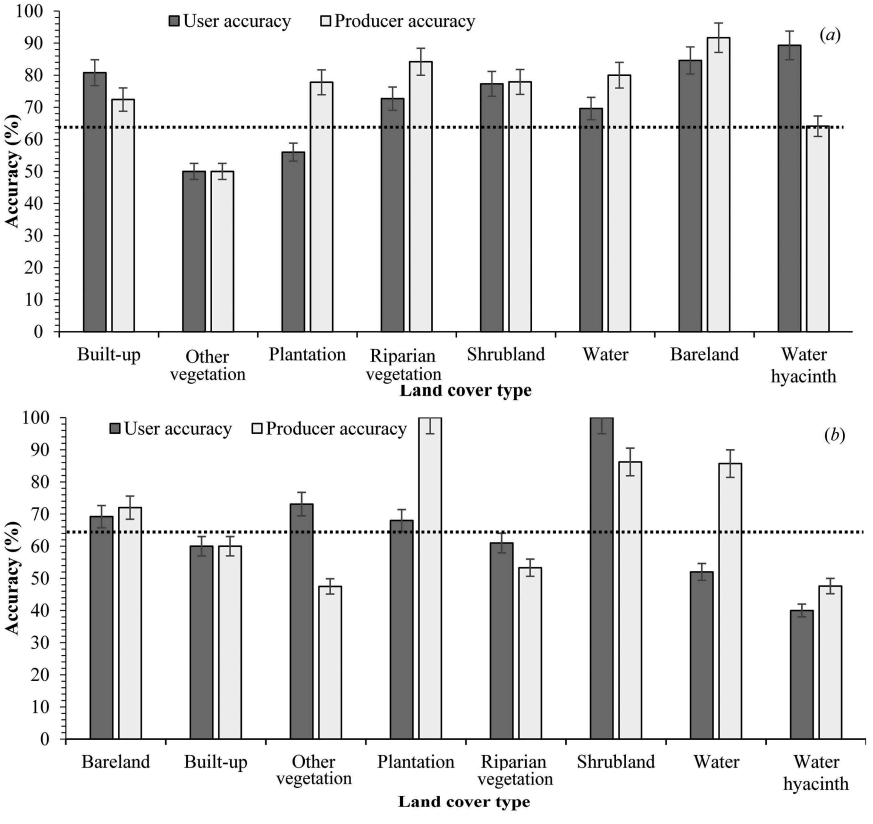

Figure 5. (a) Sentinel-2 and (b) Landsat 8 classification accuracies (%) for water hyacinth and other land-cover types using derived vegetation indices.

two sensors in mapping water hyacinth using *t*-test, and the results derived from *t*-test showed that there was significant difference ($t = 6.313$, $p < 0.04$) in their performances. The 10 m Sentinel-2 across all the analysis stages (I, II, and III) outperformed the 30 m Landsat 8 sensor.

Figure 6 illustrates the overall classification accuracies using a combined data set (spectral bands and spectral vegetation indices) derived from Landsat 8 OLI and Sentinel-2 MSI imagery.

3.3. *Capability of Landsat 8 OLI and Sentinel-2 sensors in mapping the spatial distribution of water hyacinth and other land-cover types*

Figure 8(a,b) illustrates the derived thematic maps showing land-use and land-cover revealing water hyacinth within the study area, using Landsat 8 OLI and Sentinel-2 MSI. Sentinel-2 MSI was capable of detecting and distinguishing most river portions affected by water hyacinth from other land-cover types. On the other hand, 30 m Landsat 8 OLI comparatively to Sentinel-2 MSI did not detect and map certain area infested with water hyacinth.

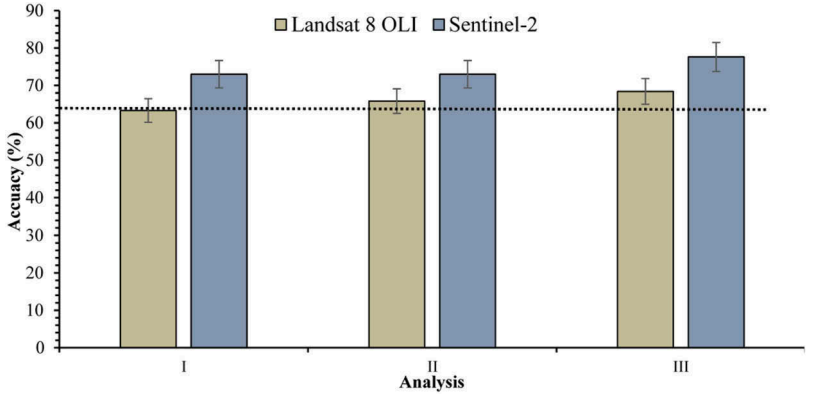

Figure 6. Combined spectral bands and spectral vegetation indices overall classification accuracies derived from Sentinel-2 MSI and Landsat 8 OLI.

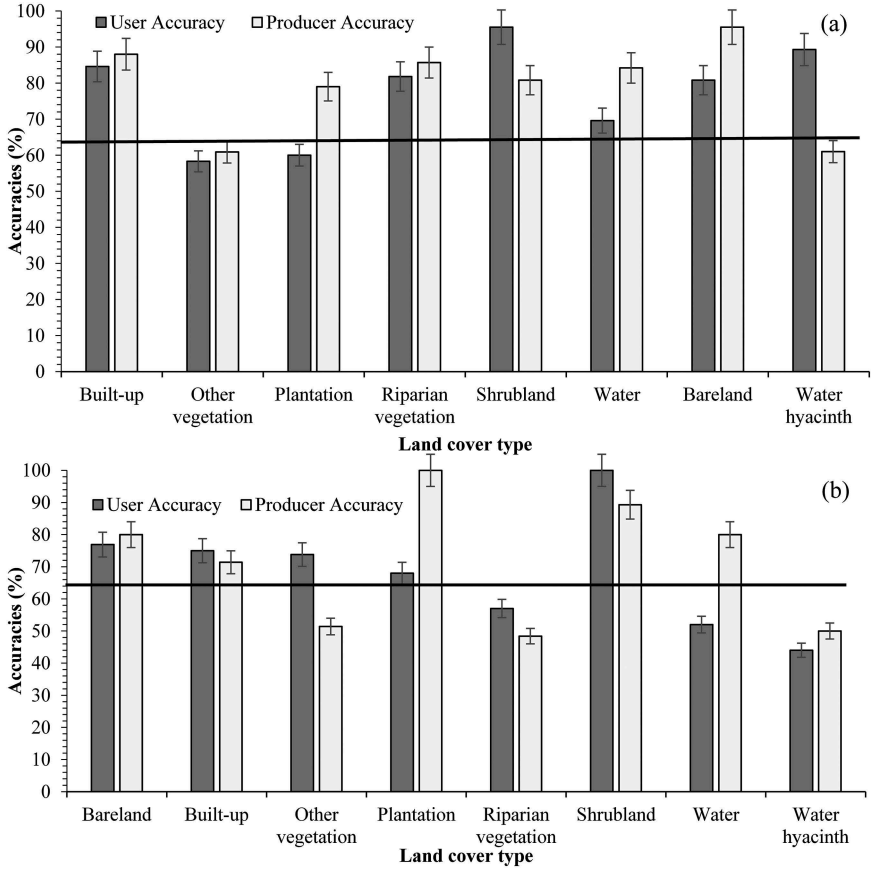

Figure 7. (a) Sentinel-2 and (b) Landsat 8 classification accuracies (%) for land-cover types using combined spectral bands and spectral vegetation indices.

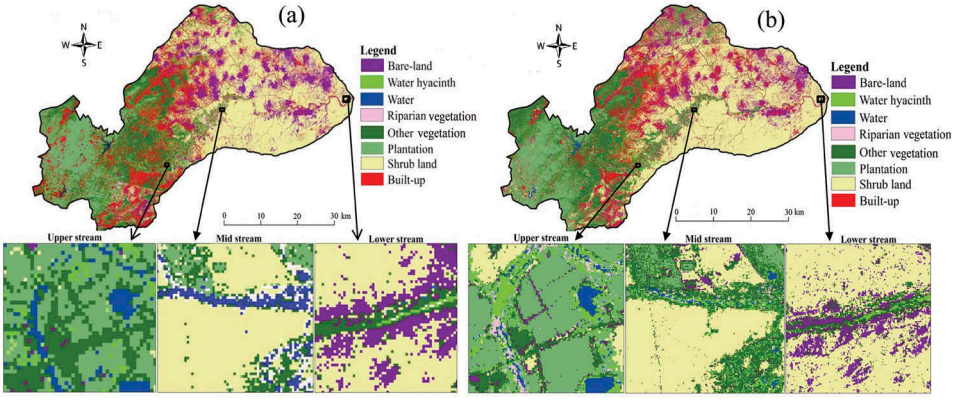

Figure 8. (a) Strength of Landsat 8 and (b) Sentinel-2 in mapping the spatial distribution of invasive water hyacinth and other land-cover types.

4. Discussion

The main aim of the study was to test the capability of new multispectral satellite data, Landsat 8 OLI and Sentinel-2 MSI sensors, in detecting and mapping the spatial distribution of water hyacinth in freshwater ecosystem. However, the study proved that Sentinel-2 MSI outperformed Landsat 8 OLI in discriminating water hyacinth from other land-cover types, such as water, plantation, built-up areas, riparian vegetation, other vegetation, shrub land, as well as bare land. Besides, detecting and mapping the spatial distribution of water hyacinth are of importance in understanding its spatial pattern and extent before removal and management practices can take place. This information is critical to aquatic scientists, environmentalists, and hydrologists, as well as catchment managers, especially in complex environments. Management practices include biological control; furthermore, derived information will guide managers on how and where to start applying practices.

The outcome of this study confirmed the capability of newly launched Sentinel-2 MSI in detecting and mapping water hyacinth in freshwater system on a river scale, when compared to Landsat 8 OLI. Using spectral band data sets of both sensors, Sentinel-2 achieved an overall classification accuracy of 73%, whereas Landsat 8 had an accuracy of 63.34%. Statistically, when compared to Sentinel-2, Landsat 8 had a magnitude of 9.66%, which clearly demonstrates the sensor's poor performance in mapping water hyacinth from riverine and other related plants. The observed performance of Sentinel-2 MSI also confirmed by the recent study by Shoko and Mutanga (2017) where they discriminated C3 and C4 grass functional types in the Drakensburg with high accuracy (85.45%). In their study, they concluded that the overall high classification was primarily attributed to the presence of more spectral bands, which provided more windows for spectral separability of specified land-cover types. In contrast to other bands, the blue, red, RE, and SWIR spectral regions played a key role in boosting spectral separability of water hyacinth from other land-cover type. The selection of these bands can be attributed to the improved and unique sensitivity to plant biophysical and chemical properties (Dube and Mutanga 2015).

Furthermore, findings of this study showed that spectral vegetation indices derived from both sensors outperformed the overall performance of raw spectral bands in discriminating water hyacinth. For instance, the use of spectral vegetation indices for Sentinel-2 MSI yielded an overall accuracy of 73.31%, whereas Landsat 8 OLI had an accuracy of 65.53%. More interestingly, Sentinel-2 MSI accuracy increased by 0.31% and by 2.19% for Landsat 8 OLI when compared to raw spectral band reflectance. These findings are in line with various observations from literature (Motangera et al., 2017; Shoko and Mutanga 2017), which shows that satellite-derived vegetation indices provide one of the best possible ways to obtain the subtle vegetation biophysical parameters. Good classification accuracies from the use of spectral vegetation indices maybe linked to the strength of the normalized difference vegetation indices (NDVI). Liu and Huete (1995), Díaz and Blackburn (2003), and Sibanda, Mutanga, and Rouget (2015) reported that the performance of vegetation indices like NDVI could be attributed to its ability to suppress background effects much better than individual spectral bands. Such background effects include atmospheric impurities, soil or shadow backgrounds, as well as zenith angle of the sensor. Moreover, the outstanding performance of Sentinel-2 MSI may be attributed to its spatial resolution, a unique spectral band setting, which together with spectral vegetation indices offers an advantageous alternative than available broadband and low spatial resolution sensors, such as Landsat data.

The combined data sets (i.e. spectral bands and spectral vegetation indices) further proved its capability in discriminating water hyacinth from other land-cover types. Although Sentinel-2 showed the supremacy in the discrimination process, both sensors produced overall classification accuracy within the range of 68.41–77.56%. Generally, Sentinel-2 MSI outperformed Landsat 8 OLI by a huge margin of 9.66%. The decrease in Landsat 8 OLI with 9.66% can be attributed to the sensor's challenges emanating from the spectral confusion of water hyacinth with other land-cover types within the study area. Considering its 30 m spatial resolution requirements in a river scale (width between 8 and 60 m), the sensor was incapable of classifying water hyacinth from other land-cover types in narrow environments. In contrary, width of the river and spatial resolution of Landsat 8 OLI resulted in the sensor's low sensitivity to water hyacinth, hence slightly lower discrimination capabilities. Therefore, the observed capability of the newly launched Sentinel-2 MSI makes it a better and future alternative in discriminating and monitoring aquatic vegetation, especially in a river system.

Overall, classification accuracies in both images increased, and this was influenced by integration of spectral bands and spectral vegetation indices. Besides, combined data set from the 10 m Sentinel-2 MSI spatial resolution enhanced the sensor's potential to discriminate water hyacinth in the river systems. In this regard, results achieved in this study concur with research finding published by Matongera et al. (2017) who reported that combining spectral bands and spectral vegetation indices significantly improved the discrimination of bracken fern weeds. In addition, the work by Sibanda, Mutanga, and Rouget (2015) also pointed on the value of combining spectral bands with spectral vegetation indices obtained from Sentinel-2 in quantifying grass above ground biomass treated with different fertilizer treatments. High results produced are due to the increased numbers of variables sensitive to plant biophysical properties.

Spatially, Sentinel-2 managed to depict the spatial distribution of water hyacinth along the course of river (upper, mid-, and lower stream). Furthermore, it can be seen in the Sentinel-2 image that in the upper and mid-stream, water hyacinth has clogged this freshwater ecosystem. These findings are in line with the observed land-use patterns within the area where it can

be observed that alongside these selected sections of river there are commercial agricultural farms practising intensive farming. However, nutrients from commercial farms contribute in eutrophication that creates a very conducive breeding ground for invasive species to thrive (Aboyeji 2013; Galadima et al. 2011; Carpenter and Biggs 2009). Furthermore, the wide spread of water hyacinth can be influenced by nutrients washed into water system through run-off, as well as sewage disposal from upstream townships (Dube et al., 2017). Sewage spillage into open waterbodies proliferates the biological oxygen strains to such a high level that all the available oxygen may be removed; subsequently, aquatic animals and even aquatic weeds can thrive or vice versa, creating momentous distraction in the food chain (Aboyeji 2013).

5. Conclusion

In this study, we tested two robust push-broom multispectral sensors: Landsat 8 and Sentinel-2 in identifying, detecting and mapping the spatial distribution and configuration of invasive water hyacinth in a river system. The findings of the study derived using DA demonstrated that newly launched Sentinel-2 outperformed Landsat 8 OLI in mapping water hyacinth, producing an overall classification accuracy of 77.56% compared to 68.44% for Landsat 8. Improved water hyacinth classification results were further observed from the integration of Sentinel-2 spectral bands and vegetation indices. Furthermore, the variable importance results demonstrated selected blue, RE 1, SWIR-1, and SWIR-2 bands as the most critical and outstanding spectral regions for detecting and mapping water hyacinth from other land-cover types. The newly launched 10 m spatial resolution Sentinel-2 MSI sensor showed enhanced capability in detecting, mapping, and monitoring the spatial distribution, configuration, and invasion magnitude of invasive water hyacinth in a river scale.

Acknowledgements

The authors are appreciative to the National Aeronautics and Space Administration for the provision of Landsat 8 OLI and Sentinel-2 MSI images with no cost attached. The authors are also thankful to Risk and Vulnerability Science Centre (RVSC) for funding the research. The authors also would like to thank Mr Sepuru T.K. and Mr Dhau I. for data collection. The authors also thank the reviewers for the comments.

Disclosure statement

No potential conflict of interest was reported by the authors.

Funding

This work was supported by the University of South African National Research Foundation (NRF) and the Risk and Vulnerability Science Centre (RVSC), University of Limpopo.

ORCID

Kgabo Humphrey Thamaga http://orcid.org/0000-0002-2305-9975
Timothy Dube http://orcid.org/0000-0003-3456-8991

References

Aboyeji, O. O. 2013. "Freshwater Pollution in Some Nigerian Local Communities, Causes, Consequences and Probable Solutions." *Academic Journal of Interdisciplinary Studies* 2 (13): 111.

Adelabu, S., O. Mutanga, E. Adam, and R. Sebego. 2014. "Spectral Discrimination of Insect Defoliation Levels in Mopane Woodland Using Hyperspectral Data." *IEEE Journal of Selected Topics in Applied Earth Observation and Remote Sensing* 7: 177–186. doi:10.1109/JSTARS.2013.2258329.

Adjorlolo, C., O. Mutanga, M. A. Cho, and R. Ismail. 2013. "Spectral Resampling Based on User-Defined Inter-Band Correlation Filter: C3 and C4 Grass Species Classification." *International Journal of Applied Earth Observation and Geoinformation* 21: 535–544. doi:10.1016/j.jag.2012.07.011.

Africa Population and Health Research Center (APHRC). 2014. *Population and Health Dynamics in Nairobi's Informal Settlements*. Report of the Nairobi Cross-sectional Slums Survey (NCSS) 2012. APHRC, Nairobi.

Albright, T. P., T. G. Moorhouse, and T. J. McNabb. 2004. "The Rise and Fall of Water Hyacinth in Lake Victoria and the Kagera River Basin," 1989–2001." *Journal of Aquatic Plant Management* 42: 73–84.

Bonansea, M., M. C. Rodriguez, L. Pinotti, and S. Ferrero. 2015. "Using Multi-Temporal Landsat Imagery and Linear Mixed Models for Assessing Water Quality Parameters in Río Tercero Reservoir (Argentina)." *Remote Sensing of Environment* 158: 28–41. doi:10.1016/j.rse.2014.10.032.

Bresciani, M., C. Giardino, M. Bartoli, S. Tavernini, R. Bolpagni, and D. Nizzoli. 2011. "Recognizing Harmful Algal Bloom Based on Remote Sensing Reflectance Band Ratio." *Journal Application of Remote Sensing* 5: 053–556.

Carpenter, S. R., and R. Biggs. 2009. "Freshwaters: Managing across Scales in Space and Time, in Principals of Ecosystem Stewardship." *Springer Science* 197–220.

Chawira, M., T. Dube, and W. Gumindoga. 2013. "Remote Sensing Based Water Quality Monitoring in Chivero and Manyame Lakes of Zimbabwe." *Physics and Chemistry of the Earth Parts A/B/C* 66: 38–44. doi:10.1016/j.pce.2013.09.003.

Cheruiyot, E. K., C. Mito, M. Menenti, B. Gorte, R. Roderik Koenders, and N. Akdim. 2014. "Evaluating MERIS-Based Aquatic Vegetation Mapping in Lake Victoria." *Remote Sensing* 6: 7762–7782. doi:10.3390/rs6087762.

Congalton, R. G. 1991. "A Review of Assessing the Accuracy of Classifications of Remotely Sensed Data." *Remote Sensing of Environment* 37: 35–46. doi:10.1016/0034-4257(91)90048-B.

Congalton, R. G., and K. Green. 1999. *Assessing the Accuracy of Remotely Sensed Data: Principles and Practices*. Boca Raton: Lewis Publishers.

DEAT. 2001. *State of the Rivers Report*. Accessed 20 February 2017. http://soer.deat.gov.za/dm_documents/LimpopoLLtf4tA.pdf

Deering, D. W., J. W. Rouse, R. H. Haas, and J. A. Schell. 1975. "Measuring 'Forage Production' of Grazing Units from Landsat MSS Data." *Proceedings of the 10th International Symposium on Remote Sensing of Environment II* 1169–1178.

Dhau, I., E. Adam, O. Mutanga, and K. K. Ayisi. 2017. "Detecting the Severity of Maize Streak Virus Infestations in Maize Crop Using *In Situ* Hyperspectral Data." *Transections of the Royal Society of South Africa* 73 (1): 8–15. doi:10.1080/0035919X.2017.1370034.

Díaz, B. M., and G. A. Blackburn. 2003. "Remote Sensing of Mangrove Biophysical Properties: Evidence from a Laboratory Simulation of the Possible Effects of Background Variation on Spectral Vegetation Indices." *International Journal of Remote Sensing* 24 (1): 53–73. doi:10.1080/01431160305012.

Dronova, I., P. Gong, and L. Wang. 2011. "Object-Based Analysis and Change Detection of Major Wetland Cover Types and Their Classification Uncertainty during the Low Water Period at Poyang Lake, China." *Remote Sensing of Environment* 115: 3220–3236. doi:10.1016/j.rse.2011.07.006.

Dube, T., and O. Mutanga. 2015. "Evaluating the Utility of the Medium-Spatial Resolution Landsat 8 Multispectral Sensor in Quantifying Aboveground Biomass in uMgeni Catchment, South Africa." *ISPRS Journal of Photogrammetry and Remote Sensing* 101: 36–46. doi:10.1016/j.isprsjprs.2014.11.001.

Dube, T., O. Mutanga, M. Sibanda, V. Bangamwabo, and C. Shoko. 2017. "Evaluating the Performance of the Newly-launched Landsat 8 Sensor in Detecting and Mapping the Spatial Configuration of Water Hyacinth (Eichhornia Crassipes) in Inland Lakes, Zimbabwe." *Physics and Chemistry of the Earth, Parts A/b/c* 100: 101–111.

Dube, T., W. Gumindoga, and M. Chawira. 2014. "Detection of Land Cover Changes around Lake Mutirikwi, Zimbambwe, Based on Traditional Remote Sensing Classification Techniques." *African Journal of Aquatic Science* 39 (1): 89–95. doi:10.2989/16085914.2013.870068.

El-Askary, H., S. Abd El-Mawla, J. Li, M. El-Hattab, and M. El-Raey. 2014. "Change Detection of Corel Reef Habitat Using Landsat-5 TM, Landsat 7 EMT+ and Landsat 8 OLI Data in the Red Sea (Hurghada, Egypt)." *International Journal of Remote Sensing* 35 (6): 2327–2346.

Fernandez, G. C. 2002. "Discrimination Analysis, a Powerful Classification Technique in Data Mining." *Proceedings of the SAS Users International Conference*, 247–256.

Foody, G. M. 2004. "Thematic Map Comparison: Evaluating the Statistical Significance of Differences in Classification Accuracy." *Photogrammetric Engineering and Remote Sensing* 70: 627–633. doi:10.14358/PERS.70.5.627.

Fu, C. 2003. "Potential Impacts of Human-Induced Land Cover Change on East Asia Monsoon." *Global Planet Change* 37: 219–229.

Galadima, A., Z. N. Garba, L. Leke, M. N. Almustapha, and I. K. Adam. 2011. "Domestic Water Pollution among Local Communities in Nigeria – Causes and Consequences." *European Journal of Scientific* 52 (4): 592–603.

Giardino, C., M. Bresciani, E. Valentini, L. Gasperini, R. Bolpagni, and V. E. Brando. 2015. "Airborne Hyperspectral Data to Assess Suspended Particulate Matter and Aquatic Vegetation in Shallow and Turbid Lake." *Remote Sensing of Environment* 157: 48–57. doi:10.1016/j.rse.2014.04.034.

Gitelson, A. A., A. Viña, V. Ciganda, D. C. Rehnquist, and T. J. Arkebauer. 2015. "Remote Estimation of Canopy Chlorophyll Content in Crops." *Geophysical Research Letters* 32: 08–403.

Gitelson, A. A., Y. J. Kaufman, and M. N. Merzlyak. 1996. "Use of a Green Channel in Remote Sensing of Global Vegetation from EOS-MODIS." *Remote Sensing of the Environment* 58: 289–298. doi:10.1016/S0034-4257(96)00072-7.

Harvey, R. M., J. R. Pickett, and R. D. Bates. 1987. "Environmental Factors Controlling the Growth and Distribution of Submersed Aquatic Macrophytes in Two South Carolina Reservoirs." *Lake and Reservoir Management* 3: 243–255. doi:10.1080/07438148709354780.

Hassan, Z., R. Shabbir, S. S. Ahmad, A. H. Malik, N. Aziz1, A. Butt, and S. Erum. 2016. "Dynamics of Land Use and Land Cover Change (LULCC) Using Geospatial Techniques: A Case Study of Islamabad Pakistan." *SpringerPlus* 5: 812. doi:10.1186/s40064-016-2414-z.

Hestir, E. L., S. Khanna, M. E. Andrew, M. J. Santos, J. H. Viers, and J. A. Greenberg. 2008. "Identification of Invasive Vegetation Using Hyperspectral Remote Sensing in the California Delta Ecosystem." *Remote Sensing of the Environment* 112: 4034–4047. doi:10.1016/j.rse.2008.01.022.

Hestir, E. L., V. E. Brando, M. Bresciani, C. Giardino, E. Matta, and P. Villa. 2015. "Measuring Freshwater Aquatic Ecosystems: The Need for a Hyperspectral Global Mapping Satellite Mission." *Remote Sensing of Environment* 167: 181–195. doi:10.1016/j.rse.2015.05.023.

Hillnhutter, C., and A. K. Mahleni. 2008. "Early Detection and Localisation of Sugar Beet Diseases." *New Approaches Gesunde Pflanzen* 60 (4): 143–149.

Hou, X., L. Feng, H. Duan, X. Chen, D. Sun, and K. Shi. 2017. "Fifteen-Year Monitoring of the Turbidity Dynamics in Large Lakes and Reservoirs in the Middle and Lower Basin of the Yangtze River, China." *Remote Sensing of Environment* 190: 107–121. doi:10.1016/j.rse.2016.12.006.

Huang, C., Y. Peng, M. Lang, I. Y. Yeo, and G. McCarty. 2014. "Wetland Inundation Mapping and Change Monitoring Using Landsat and Airborne LiDAR Data." *Remote Sensing of Environment* 141: 231–242. doi:10.1016/j.rse.2013.10.020.

Huete, A., H. Liu, K. V. Batchily, and W. Van Leeuwen. 1997. "A Comparison of Vegetation Indices over a Global Set of TM Images for EOS-MODIS." *Remote Sensing of the Environment* 59: 440–451. doi:10.1016/S0034-4257(96)00112-5.

Huete, A. R. 1988. "A Soil-Adjusted Vegetation Index (SAVI)." *Remote Sensing of the Environment* 25: 295–309. doi:10.1016/0034-4257(88)90106-X.

Jin, H., C. Huang, M. W. Lang, I. Y. Yeo, and V. S. Stehman. 2017. "Monitoring of Wetland Inundation Dynamics in the Delmarva Peninsula Using Landsat Time-Series Imagery from 1985 to 2011." *Remote Sensing of Environment* 190: 26–41. doi:10.1016/j.rse.2016.12.001.

Jordan, C. F. 1969. "Derivation of Leaf-Area Index from Quality of Light on the Forest Floor." *Ecology* 50: 663–666. doi:10.2307/1936256.

Kaufman, Y. J., and D. Tanré. 1992. "Atmospherically Resistant Vegetation Index (ARVI) for EOS-MODIS." *IEEE Transactions on Geoscience and Remote Sensing* 30 (2): 261–270. doi:10.1109/36.134076.

Kaufmann, R. K., and D. I. Stern. 1997. "Evidence for Human Influence on Climate from Hemispheric Temperature Relations." *Nature* 388: 39–44. doi:10.1038/40332.

Krishna, A., M. Siram, and P. Prakash. 2014. "Slum Types and Adaptation Strategies: Identifying Policy-Relevant Differences in Bangalore." *Environment and Urbanization* 26 (2): 568–585. doi:10.1177/0956247814537958.

Lamaro, A. A., A. Mariñelarena, and S. E. Torrusio. 2013. "Water Surface Temperature Estimate from Landsat 7 ETM+ Thermal Infrared Data Using the Generalized Single-Channel Method: Case Study of Embalse Del Rió Tercero (Córdoba, Argentina)." *Advanced in Space Research* 51 (3): 492–500. doi:10.1016/j.asr.2012.09.032.

Li, L., Y. Chen, T. Xu, R. Liu, K. Shi, and C. Huang. 2015. "Super-Resolution Mapping of Wetland Inundation from Remote Sensing Imagery Based on Integration of Back-Propagation Neural Network and Genetic Algorithm." *Remote Sensing of Environment* 164: 142–154. doi:10.1016/j.rse.2015.04.009.

Liu, H. Q., and A. Huete. 1995. "A Feedback Based Modification of the NDVI to Minimize Canopy Background and Atmospheric Noise." *IEEE Transactions on Geoscience and Remote Sensing* 33 (2): 457–465. doi:10.1109/36.377946.

Masocha, M., A. Murwira, C. H. D. Magadza, R. Hirji, and T. Dube. 2017. "Remote Sensing of Surface Water Quality in Relation to Catchment Condition in Zimbabwe." *Physics and Chemistry of the Earth* 100: 1–6.

Matongera, T. N., O. Mutanga, T. Dube, and M. Sibanda. 2017. "Detection and Mapping the Spatial Distribution of Bracken Fern Weeds Using the Landsat 8 OLI New Generation Sensor." *International Journal of Applied Earth Observation and Geoformation* 57: 93–103. doi:10.1016/j.jag.2016.12.006.

McFeeters, S. K. 1996. "The Use of the Normalized Difference Water Index (NDWI) in the Delineation of Open Water Features." *International Journal of Remote Sensing* 17: 1425–1432. doi:10.1080/01431169608948714.

McMullough, I. M., C. S. Loftion, and S. A. Sader. 2012. "High Frequency Remote Monitoring of Large Lakes with MODIS 500 M Imagery." *Remote Sensing of Environment* 124: 234–241. doi:10.1016/j.rse.2012.05.018.

Mendes, A. P. F., M. A. Bertella, and F. A. P. Teixeira. 2014. "Industrialization in Sub-Saharan Africa and Import Substitution Policy." *Brazilian Journal of Political Economy* 34: 1. doi:10.1590/S0101-31572014000100008.

Midgley, G. F., R. A. Chapman, B. Hewitson, P. Johnston, M. De Wit, G. Ziervogel, P. Mukheibir, et al. 2005. *A Status Quo, Vulnerability and Adaptation Assessment of the Physical and Socio-Economic Effects of Climate Change in the Western Cape*. Report to the Western Cape Government, Cape Town, South Africa. CSIR Report No. ENV-S-C 2005-073, Stellenbosch.

Pahlevan, N., and J. R. Schott. 2013. "Leverage EO-1 to Evaluate Capability of New Generation of Landsat Sensors for Coastal/Inland Water Studies." *IEEE Journal Selected Topics in Applied Earth Observations and Remote Sensing* 6 (2): 360–374. doi:10.1109/JSTARS.2012.2235174.

Panetta, F. D., and R. Lawes. 2005. "Evaluation of the Performance of Weed Eradication Programs: The Delimitation of Extent." *Diversity and Distributions* 11: 435–442. doi:10.1111/j.1366-9516.2005.00179.x.

Pearsall, W. H. 1920. "The Aquatic Vegetation of English Lakes." *Journal of Ecology* 8 (3): 163–201. doi:10.2307/2255612.

Peerbhay, K. Y., O. Mutanga, and R. Ismail. 2016. "The Identification and Remote Detection of Alien Invasive Plants in Commercial Forest: An Overview." *South African Journal of Geomatics* 5: 1.

Potts, D. 2013. Rural–Urban and Urban–Rural Migration Flows as Indicators of Economic Opportunity in Sub-Saharan Africa: What Do the Data Tell Us? Migrating Out of Poverty Working Paper 9. *Migrating Out of Poverty Consortium*, University of Sussex, Brighton.

Rigg, J., T. Nguyen, and T. Luong. 2014. "The Texture of Livelihoods: Migration and Making a Living in Hanoi." *The Journal of Development Studies* 50 (3): 368–382. doi:10.1080/00220388.2013.858130.

Rondeaux, G., M. Steven, and F. Baret. 1996. "Optimization of Soil-Adjusted Vegetation Indices." *Remote Sensing of Environment* 55: 95–107. doi:10.1016/0034-4257(95)00186-7.

Rorslett, B. 1984. "Environmental Factors and Aquatic Macrophyte Response in Regulated Lakes." *Aquatic Botany* 19: 199–220. doi:10.1016/0304-3770(84)90039-1.

Roujean, J. L., and F. M. Breon. 1995. "Estimating PAR Absorbed by Vegetation from Bidirectional Reflectance Measurements." *Remote Sensing of Environment* 51: 375–384. doi:10.1016/0034-4257(94)00114-3.

Shekede, M., S. Kusangaya, and K. Schmidt. 2008. "Spatio-Temporal Variations of Aquatic Weeds Abundance and Coverage in Lake Chivero, Zimbabwe." *Physics and Chemistry of the Earth, Parts A/B/C* 33: 714–721. doi:10.1016/j.pce.2008.06.052.

Shoko, C., and O. Mutanga. 2017. "Examining the Strength of the Newly-Launched Sentinel 2 MSI Sensor in Detecting and Discriminating Subtle Differences between C3 and C4 Grass Species." *ISPRS Journal of Photogrammetry and Remote Sensing* 129: 32–40. doi:10.1016/j.isprsjprs.2017.04.016.

Sibanda, M., O. Mutanga, and M. Rouget. 2015. "Examining the Potential of Sentinel-2 MSI Spectral Resolution in Quantifying Above Ground Biomass across Different Fertilizer Treatments." *ISPRS Journal Photogrammetry of Remote Sensing* 110: 55–65. doi:10.1016/j.isprsjprs.2015.10.005.

Sripada, R. P., R. W. Heiniger, J. G. White, and A. D. Meijer. 2006. "Aerial Color Infrared Photography for Determining Early In-Season Nitrogen Requirements in Corn." *Agronomy Journal* 98: 968–977. doi:10.2134/agronj2005.0200.

Sriwongsitanon, N., K. Surakit, and S. Thianpopirug. 2011. "Influence of Atmospheric Correction and Number of Sampling Points on the Accuracy of Water Clarity Assessment Using Remote Sensing Application." *Journal of Hydrology* 401 (3–4): 203–220. doi:10.1016/j.jhydrol.2011.02.023.

Tebbs, E. J., J. J. Remedios, and D. M. Happer. 2013. "Remote Sensing of Chlorophyll-A as a Measure of Cyanobacterial Biomass in Lake Bogoria, a Hypertrophic, Saline-Alkaline, Flamingo Lake, Using Landsat 7 ETM+." *Remote Sensing of Environment* 135: 92–106. doi:10.1016/j.rse.2013.03.024.

Tucker, C. J. 1979. "Red and Photographic Infrared Linear Combinations for Monitoring Vegetation." *Remote Sensing of the Environment* 8: 127–150. doi:10.1016/0034-4257(79)90013-0.

Yavaşl, D. D. 2016. "Estimation of above Ground Forest Biomass at Muğla Using ICESat/GLAS and Landsat Data." *Remote Sensing Applications: Society and Environment* 4: 211–218.

Zarco-Tejada, P. J., A. Berjón, R. López-Lozano, J. R. Miller, P. Martín, V. Cachorro, M. R. González, and A. De Frutos. 2005. "Assessing Vineyard Condition with Hyperspectral Indices: Leaf and Canopy Reflectance Simulation in a Row-Structured Discontinuous Canopy." *Remote Sensing of Environment* 99: 271–287. doi:10.1016/j.rse.2005.09.002.

Zhang, X., S. Wu, X. Yan, and Z. Chen. 2016. "A Global Classification of Vegetation Based on NDVI, Rainfall and Temperature." *International Journal of Climatology* 37 (5): 2018–2324.